Scientia Iranica B (2015) 22(1), 245–257

SCIENTIA IRANICA

Sharif University of Technology
Scientia Iranica
Transactions B: Mechanical Engineering
www.scientiairanica.com

Energy and exergy analysis and optimization of a μ-solar-driven combined ejector-cooling and power system based on organic Rankine cycle using an evolutionary algorithm

F.A. Boyaghchi* **and P. Heidarnejad**

Department of Mechanical Engineering, Faculty of Engineering & Technology, Alzahra University, Deh-Vanak, Tehran, P. Code: 1993893973, Iran.

Received 7 December 2013; received in revised form 25 May 2014; accepted 29 September 2014

KEYWORDS
Energy;
Exergy;
CECP;
Ejector;
Optimization;
GA.

Abstract. This paper proposes and investigates a Combined Ejector-Cooling and Power (CECP) system, using R123 as a working fluid to utilize the solar energy over a low temperature range. Evacuated tube solar collectors are used to collect the solar radiation for their low costs. A thermal storage system and an auxiliary boiler are used to provide continuous cooling and power output when solar radiation is not sufficient. Mathematical models are employed to simulate the system under steady-state conditions. The results obtained reveal that solar collector and auxiliary boiler are the main exergy destruction sources. Parametric analysis is conducted to examine the effects of some key thermodynamic parameters on the system performance. The results indicate that under the actual constraints, increasing turbine inlet pressure elevates system efficiency while increasing turbine inlet temperature and turbine back pressure decreases that. The system is also optimized with the energy and exergy efficiencies as objective functions by means of genetic algorithm under the given conditions.

1. Introduction

Low temperature waste heat and renewable energies, such as solar and geothermal energies as low temperature heat sources are discussed extensively in the literature. These energies cannot be employed in the conventional power plants efficiently. Recently, various and refrigeration cogeneration and power cycles have been proposed to utilize them in energy-efficient systems. Goswami [1] proposed refrigeration cogeneration and power system for the low temperature heat sources ($< 200^{\circ}C$). The proposed cycle integrated with the Rankine cycle and the absorption refrigeration cycle. Many researchers [2-10] investigated the Goswami's proposed cycle both theoretically and experimentally. They found that the combined cycle proposed is suitable for utilizing the low temperature heat sources efficiently. However, the refrigeration capacity of the proposed cycle is relatively small, because the phase of the working fluid does not change during the refrigeration process. Various systems based on the combined power and absorption refrigeration cycle were provided by other researchers. Amano et al. [11,12] provided a hybrid power and refrigeration cycle that combined an ammonia-water power cycle and an absorption refrigeration cycle. The power cycle provided stronger solution to the refrigeration cycle rectifier to elevate

*. *Corresponding author. Tel.: +98 21 88044040-2140; Fax: +98 21 88617537*
E-mail addresses: fahmadi@alzahra.ac.ir (F.A. Boyaghchi); parisaheidarnejad@yahoo.com (P. Heidarnejad)

refrigeration cycle performance. Zheng et al. [13,14] proposed a combined cycle using the cold water to decrease the condensing temperature of the Rankine cycle. Zhang et al. [15-18] proposed two combined power/refrigeration binary fluid systems driven by the exhaust gas of a gas turbine: the parallel connected system and the series connected system. In the parallel system, and in the power subsystem, the concentration of working fluid was fairly low, and the temperature match in the evaporation process was unsatisfactory. Moreover, Nord et al. [19] provided a Solar Integrated Thermal Management and Power (SITMAP) cycle, which integrates a jet pump instead of the compressor in vapor compression and a Rankine cycle. This cycle is designed for the spacecraft and driven by the solar energy collecting the solar radiation using a concentration solar collector. Overall mass system is chosen as the objective function to be minimized. Wang et al. [20] analyzed and simplified Zhang's parallel connected system in Ref. [15] to make it better for low-temperature heat sources. They eliminated the recuperator, high-pressure pump, and condenser in the power generation cycle. However, the turbine outlet steam still reached 97°C, and a large exergy loss occurred during the absorption-condensation process. Wang et al. [21] improved their cycle by applying an ejector between the condenser and rectifier. However, the plant exergy efficiency was improved by only 0.6% and the heat loss in the turbine was not recovered. Jawahar et al. [22] proposed a combined cooling and power cycle by introducing an expander into the generator absorber heat exchanger cooling cycle (GAX cycle). The expander is applied between the absorber and High-Pressure-Generator-Absorber-exchanger (HPGAX). The cooling and power cogeneration cycles are parallel, using the same vapor from the HPGAX.

This study thus aims to (1) propose a combined ejector cooling and power system driven by solar energy; (2) evaluate the thermodynamic performance of the proposed system; (3) identify the main sources of exergy destruction components; (4) study the key parameters on system performance; and (5) optimize the energetic and exergetic efficiencies of cycle using the Genetic Algorithm (GA).

2. System description

The CECP system proposed in this study is divided into two subsystems: Organic Rankine Cycle (ORC) subsystem and solar collector subsystem. Figure 1 illustrates schematic diagram of this system.

2.1. Organic rankine cycle subsystem

ORC subsystem consists of a turbine (Tur), an ejector (Ejc), two evaporators (Eva), a condenser (Con), a pump (p), an economizer (Eco) and a super heater

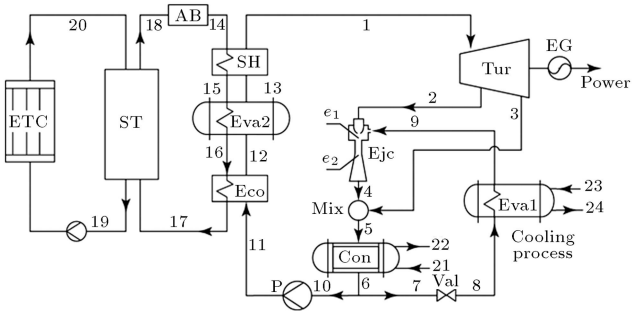

Figure 1. Schematic diagram of CECP system.

(SH). The saturated liquid is pumped into economizer and, after superheating in super heater, produces power in the turbine connected to the electric generator. The extracted vapor of the turbine enters the supersonic nozzle of ejector. The very high velocity vapor at the exit of the nozzle produces a high vacuum at the inlet of the mixing chamber and entrains secondary vapor into the chamber from the evaporator. The two streams are mixed in the mixing chamber. Then the mixed stream becomes a transient supersonic stream. One entering the constant cross-section zone, a normal shock wave occurs, accompanied by a significant pressure rise. After the shock, the velocity of the mixed stream becomes subsonic and decelerates in the diffuser. The outlet stream from ejector is mixed with turbine outlet in mixer (Mix) and discharged to the condenser to convert to liquid by rejecting heat to cooling water.

2.2. Solar collector subsystem

The major components of solar collector subsystem are an evacuated tube solar collector, thermal Storage Tank (ST) and Auxiliary Boiler (AB). The main energy source of the whole system is evacuated tube solar collector. The auxiliary boiler is installed as the backup energy source and it is used when the temperature of the thermal storage is lower than allowable temperature; on the other hand, thermal storage is used when solar radiation is insufficient. Evacuated tube solar collector for its low cost and easy installation is used.

3. Simulation and analysis of the systems

Thermodynamic modeling of the solar CECP system has been conducted based on simulation code in Engineering Equation Solver (EES) [23].

3.1. Assumptions

For simplifying the theoretical analysis following assumptions are made:

1. The system reaches a steady state, and pressure drops in pipes, vapor generator, evaporator and heat exchanger are neglected.
2. The flow across the throttle valve is isenthalpic.

3. The condenser outlet state is saturated liquid, and outlet state of evaporator is saturated vapor.
4. The pumps and the turbine have a given isentropic efficiencies.
5. All of the potential and kinetic exergies are ignored.
6. The fuel injected to the auxiliary boiler is natural gas.

3.2. Thermodynamic analysis

In order to simulate the system, the principles of mass and energy conservation are used. Neglecting the kinetic and potential energies, the general equations of these principles for a steady state process are specified as [24]:

- Mass conservation:

$$\sum m_i = \sum m_e. \tag{1}$$

- Energy conservation:

$$\sum Q - \sum W = \sum m_e h_e - \sum m_i h_i. \tag{2}$$

Here, Q denotes the heat transfer rate and W the work transfer rate. These equations are applied to each component of the systems.

3.2.1. Organic Rankine Cycle (ORC) subsystem

ORC subsystem includes turbine, two evaporators, two pumps, heater, economizer, super heater, condenser, two mixers, valve and ejector. The conservation of mass and energy principle applied to each component can be expressed as follows:

Tur:

$$m_1 = m_2 + m_3, \tag{3}$$

$$W_{\text{Turb}} = m_1 h_1 - (m_2 h_2 + m_3 h_3), \tag{4}$$

$$\eta_{\text{is,Turb}} = \frac{W_{\text{Turb}}}{W_{\text{is,Turb}}}. \tag{5}$$

Eva1:

$$m_8 = m_9, \tag{6}$$

$$Q_{CL} = m_8(h_9 - h_8). \tag{7}$$

Eva2:

$$m_{12} = m_{13}, \tag{8}$$

$$m_{15} = m_{16}, \tag{9}$$

$$m_{12}(h_{13} - h_{12}) = m_{15}(h_{15} - h_{16}). \tag{10}$$

P:

$$m_{11} = m_{10}, \tag{11}$$

$$W_p = m_{10}\nu_{10}(P_{11} - P_{10})/\eta_{\text{is},p}. \tag{12}$$

Eco:

$$m_{11} = m_{12}, \tag{13}$$

$$m_{16} = m_{17}, \tag{14}$$

$$m_{11}(h_{12} - h_{11}) = m_{16}(h_{16} - h_{17}). \tag{15}$$

SH:

$$m_{13} = m_1, \tag{16}$$

$$m_{14} = m_{15}, \tag{17}$$

$$m_{13}(h_1 - h_{13}) = m_{14}(h_{14} - h_{15}). \tag{18}$$

Con:

$$m_5 = m_6, \tag{19}$$

$$Q_{\text{Cond}} = m_5(h_5 - h_6). \tag{20}$$

Mix:

$$m_3 + m_4 = m_5, \tag{21}$$

$$m_3 h_3 + m_4 h_4 = m_5 h_5. \tag{22}$$

Val:

$$m_7 = m_8, \tag{23}$$

$$h_7 = h_8. \tag{24}$$

Ejector is the significant component in this system, and its performance is dependent upon entrainment ratio which determines the magnitude of mass flow rate of secondary refrigerant in terms of mass flow rate of primary refrigerant coming out from the turbine. Its model has been carried out based on the one-dimensional constant pressure model which is used by most researchers [25,26]. Some assumptions to model the ejector are as follows:

1. The working fluid and the second fluid will not mix until they reach the mixing chamber;
2. The velocity of the fluid into ejector and the velocity of the fluid out of diffuser are neglected, because they are much lower than the velocity of the fluid in mixing chamber;
3. The working fluid flow is one-dimensional and flow is steady state;

4. The kinetic energy at the inlets of primary and suction ports and the exit of diffuser are negligible;
5. The inner wall of the ejector is adiabatic;
6. For simplicity in deriving the model, the effects of frictional and mixing losses are taken into account by using isentropic efficiencies and needs to be determined experimentally. The efficiencies of nozzle, mixing and diffuser sections efficiencies are assumed to be 0.9, 0.85 and 0.85, respectively [25,26];
7. Mixing is assumed to occur at constant pressure over a short distance in the mixing chamber.

Based on above assumptions, mass and energy equations and detailed mathematical model for ejector are given by [27]:

$$m_2 + m_9 = m_4, \tag{25}$$

$$m_2 h_2 + m_9 h_9 = m_4 h_4. \tag{26}$$

It is known that the performance of ejector is evaluated by its entrainment ratio, μ, and given as:

$$\mu = \frac{m_9}{m_2}, \tag{27}$$

$$\mu = \sqrt{\eta_n \eta_m \eta_{\text{dif}}(h_2 - h_{e1,s})/(h_{4,s} - h_{e2})} - 1. \tag{28}$$

When the inlet state parameters of primary flow, secondary flow and back pressure of the ejector are given, the value of entrainment ratio μ could be found using iterative calculation.

3.2.2. Solar collector subsystem

The useful heat gained by solar collector, Q_u is calculated from the heat balance in the solar collector [28]:

$$Q_u = \eta_{\text{Coll}} \times A_{\text{Coll}} \times G_t, \tag{29}$$

where η_{Coll} is defined as the ratio of the useful heat gain to the incident solar radiation. Solar collector efficiency can be calculated using the following thermal performance equations [29]:

$$\eta_{\text{Coll}} = \eta_o - \left(\frac{T_a - T_0}{G_t}\right) \times a_1 - \left(\frac{(T_a - T_0)^2}{G_t}\right) \times a_2. \tag{30}$$

a_1 and a_2 are the heat loss coefficient and is adopted from product specification sheet of the selected collector [30]. To predict the performance of a solar system, instantaneous values of radiation (G_t) are required. The total instantaneous solar radiation on tilted surface is obtained from the relations [28]:

$$G_t = G_b R_b + G_d R_d + (G_b + G_d) R_R, \tag{31}$$

$$G_b = G - G_d. \tag{32}$$

R_b, R_d and R_R are calculated from [28]:

$$R_b = \frac{\sin\delta \sin(L-\beta) + \cos\delta \cosh\cos(L-\beta)}{\sin L \sin\delta + cosL \cos\delta \cos(\omega)}, \tag{33}$$

$$R_d = \frac{1 + \cos\beta}{2}, \tag{34}$$

$$R_R = \rho\left(\frac{1 - \cos\beta}{2}\right). \tag{35}$$

The diffuse to total radiation ratio for a horizontal surface is expressed with the equation [28]:

$$\frac{\bar{H}_d}{\bar{H}} = 1.311 - 3.022\bar{K}_T + 3.427\bar{K}_T^2 - 1.821\bar{K}_T^3. \tag{36}$$

For extracting hourly values from daily values, two correlations are usually used:

Liu and Jordan correlation [28]:

$$r_d = \left(\frac{\pi}{24}\right) \frac{\cos(\omega) - \cos(\omega_{ss})}{\sin(\omega_{ss}) - \left(\frac{2\pi\omega_{ss}}{360}\right)\cos(\omega_{ss})}. \tag{37}$$

Collares Pereira and Rabl correlation [28]:

$$r = \frac{\pi}{24}(\alpha + \beta\cos(\omega)) \frac{\cos(\omega) - \cos(\omega_{ss})}{\sin(\omega_{ss}) - \left(\frac{2\pi\omega_{ss}}{360}\right)\cos(\omega_{ss})}, \tag{38}$$

$$\alpha = 0.409 + 0.5016\sin(\omega_{ss} - 60),$$

$$\beta = 0.6609 - 0.4767\sin(\omega_{ss} - 60).$$

In this system, we use a sensible thermal storage system to store the collected solar energy. To simplify the model, it is assumed that the water in the insulated water storage tank is completely mixed with the water following back into the tank from the collector and the economizer. Moreover, we assume that the ambient temperature T_0 is constant and the loss of the water tank is considered. The equation for the energy balance in the tank is then [31]:

$$m_{20} c_p (T_{20} - T_{19}) = m_{17} c_p (T_{18} - T_{17}) + Q_{L,ST}. \tag{39}$$

Mass and energy equations for auxiliary heater are:

$$m_{18} = m_{14}, \tag{40}$$

$$m_f LHV_f \eta_{AB} = m_{18} c_p (T_{14} - T_{18}), \tag{41}$$

$$Q_{AB} = m_f LHV_f \eta_{AB}. \tag{42}$$

Overall system:

$$W_{\text{elec}} = (W_{\text{Turb}} - W_p) \times \eta_{\text{gen}}, \tag{43}$$

$$\eta_{\text{CECP}} = \frac{W_{\text{elec}} + Q_{CL}}{Q_u + Q_{AB}}, \tag{44}$$

$$\mathrm{SF} = \frac{Q_u}{Q_u + Q_{AB}}. \quad (45)$$

Exergy is the maximum work which can be obtained from a given form of energy using the environmental parameters as the reference state [32]. In the other words, it is an attribute of the system and environment together. In the absence of nuclear, magnetic, electrical and surface tension effects, the total exergy of a system X can be divided into four components: physical exergy, X_{PH}, kinetic exergy, X_{KN}, potential exergy, X_{PT}, and chemical exergy, X_{CH} [33]:

$$X = X_{PH} + X_{KN} + X_{PT} + X_{CH}. \quad (46)$$

In this study, the kinetic and potential exergy are assumed to be negligible as the elevation and speed have negligible changes. Applying the first and the second law of thermodynamics, the exergy balance is obtained as [34]:

$$X_Q + \sum_i m_i x_i = \sum_e m_e x_e + X_W + X_D, \quad (47)$$

$$X_Q = \left(1 - \frac{T_0}{T}\right) Q, \quad (48)$$

$$X_W = W, \quad (49)$$

where X_Q and X_W are the corresponding exergy of heat transfer and work which across the boundaries of the control volume. The exergy destruction rate and the exergy efficiency for each component for the whole system are shown in Table 1.

The exergy inputs to the system come from sun and natural gas, which is used in auxiliary boiler, given for sun as [35]:

$$X_s = G_t A_{\mathrm{Coll}} \left(1 + \frac{1}{3}\left(\frac{T_0}{T_s}\right)^4 - \frac{4}{3}\left(\frac{T_0}{T_s}\right)\right), \quad (50)$$

in which T_s is taken to be 6000 K, and:

$$X_f = m_f x_f, \quad (51)$$

for natural gas, in which x_f is considered to be 51393 kJ kg^{-1}.

4. Inputs of the system simulation

Simulation of the solar CECP system is conducted based on some inputs which are shown in Table 1. R123 is selected as working fluid because it could prove to be the suitable working fluid for ORC system due to its high system performance and low operating pressure. Moreover it is nontoxic, nonflammable and non-corrosive [31,36]. The Ozone Depletion Potential (ODP) and Global Warning Potential (GWP) of R123 are 0.020 and 77 years respectively [31]. Water is used as medium in evacuated solar collector and as storage liquid in heat storage tank.

In this study, electricity, cooling and heating load of a hypothetical one-floor building which is located in Urmia city (37.4N, 45.3E), Iran, is calculated. Urmia temperature is variable between -6.32°C and 25.87°C in a year and maximum and minimum daily insolation on a horizontal surface is 9.13 and 0.83 kWh m^{-2} day^{-1} [37]. The modeling is conducted based on maximum and minimum daily insolation incident on horizontal surface which occurs on July 17th. Monthly average insolation incident on horizontal surface value is shown in Table 2.

The required collector area is specified based on meteorological data extracted from NASA internet site [37].

Table 1. Exergy destruction rate and efficiency for system components.

Component	Exergy destruction rate	Exergy efficiency
Tur	$X_{D,\mathrm{Tur}} = m_1 x_1 - m_2 x_2 - m_3 x_3 - W_{\mathrm{Turb}}$	$\varepsilon_{\mathrm{Tur}} = 1 - \frac{X_{D,\mathrm{Tur}}}{m_1 x_1 - m_2 x_2 - m_3 x_3}$
Ejc	$X_{D,\mathrm{Ejc}} = m_2 x_2 + m_9 x_9 - m_4 x_4$	$\varepsilon_{\mathrm{Ejc}} = 1 - \frac{X_{D,\mathrm{Ejc}}}{m_2 x_2 + m_9 x_9}$
Eva1	$X_{D,\mathrm{Eva1}} = m_8 x_8 + m_{23} x_{23} - m_9 x_9 - m_{24} x_{24}$	$\varepsilon_{\mathrm{Eva1}} = 1 - \frac{X_{D,\mathrm{Eva1}}}{m_8 x_8 + m_{23} x_{23}}$
Eva2	$X_{D,\mathrm{Eva2}} = m_{15} x_{15} + m_{12} x_{12} - m_{16} x_{16} - m_{13} x_{13}$	$\varepsilon_{\mathrm{Eva2}} = 1 - \frac{X_{D,\mathrm{Eva2}}}{m_{15} x_{15} + m_{12} x_{12}}$
P	$X_{D,\mathrm{p}} = W_p + m_{10} x_{10} - m_{11} x_{11}$	$\varepsilon_p = 1 - \frac{X_{D,p}}{W_p}$
Eco	$X_{D,\mathrm{Eco}} = m_{16} x_{16} + m_{11} x_{11} - m_{12} x_{12} - m_{17} x_{17}$	$\varepsilon_{\mathrm{Eco}} = 1 - \frac{X_{D,\mathrm{Eco}}}{m_{16} x_{16} + m_{11} x_{11}}$
SH	$X_{D,\mathrm{SH}} = m_{14} x_{14} + m_{13} x_{13} - m_{15} x_{15} - m_1 x_1$	$\varepsilon_{\mathrm{SH}} = 1 - \frac{X_{D\mathrm{SH}}}{m_{13} x_{13} + m_{14} x_{14}}$
Con	$X_{D,\mathrm{Con}} = m_5 x_5 + m_{21} x_{21} - m_6 x_6 - m_{22} x_{22}$	$\varepsilon_{\mathrm{Con}} = 1 - \frac{X_{D,\mathrm{Con}}}{m_5 x_5 + m_{21} x_{21}}$
AB	$X_{D,\mathrm{AB}} = X_f + m_{18} x_{18} - m_{14} x_{14}$	$\varepsilon_{\mathrm{AB}} = 1 - \frac{X_{D\mathrm{AB}}}{X_f}$
ST	$X_{D,\mathrm{ST}} = m_{20} x_{20} + m_{17} x_{17} - m_{18} x_{18} - m_{19} x_{19} - X_{L,\mathrm{ST}}$	$\varepsilon_{\mathrm{ST}} = 1 - \frac{X_{D\mathrm{ST}} + X_{L\mathrm{ST}}}{m_{20} x_{20} + m_{17} x_{17}}$
ETC	$X_{D,\mathrm{ETC}} = X_s + m_{19} x_{19} - m_{20} x_{20}$	$\varepsilon_{\mathrm{ETC}} = 1 - \frac{X_{D\mathrm{ETC}}}{X_s}$
CECP	$X_{D,\mathrm{CECP}} = X_s + X_f + X_{\mathrm{Eva1}} - W_{\mathrm{elec}} - X_{\mathrm{Con}} - X_{L,ST}$	$\varepsilon_{D,\mathrm{CECP}} = \frac{W_{\mathrm{elec}} + X_{\mathrm{Eva1}}}{X_s + X_f}$

Table 2. Input data for the system.

ORC subsystem	
Dead state temperature	15°C
Dead state pressure	100 kPa
Turbine inlet pressure	1000 kPa
Turbine inlet temperature	130°C
Ejector back pressure	91.48 kPa
mass flow extraction ratio	0.5
Turbine isentropic efficiency	0.85
Evaporation temperature	-5°C
Pump isentropic efficiency	0.7
Cooling water inlet pressure	300 kPa
Cooling water inlet temperature	15°C
Cooling water mass flow	0.4 kg s^{-1}
Cooling load	4.5 kW
Heating load	-
Power	2.7 kW
Electrical generator efficiency	0.95
Pinch point temperature difference	5°C
Solar subsystem	
Monthly average insolation, $\bar{H}$	28.5 MJ m^{-2} day^{-1}
Monthly averaged insolation clearness index, $\bar{K}_T$	0.7
Tilt angle (°)	37.4
Optical efficiency, η_0	0.656
Coefficient, a_1	1.4 W m^{-1} K^{-1}
Coefficient, a_2	0.007 W m^{-1} K^{-1}

5. Results

Before starting this section, the model suggested in this study was validated with the model presented elsewhere [38]. Validation has been conducted by comparison of some important parameters such as mass flow rate, temperature and pressure as shown in Table 3. As illustrated in the table, model validation against Ref. [38] has shown a good agreement for selected points. Normalized root-mean-square deviation for mass flow rate, temperature and pressure of selected points was calculated and achieved 0.12%, 5.6% and 1.72%, respectively.

In this section, the result of energy and exergy modeling of the proposed CECP system are presented and discussed. In this study, the effects of the turbine inlet pressure, turbine inlet temperature and turbine back pressure on system efficiencies and components exergy destruction rates are examined and discussed. Solar collector, auxiliary boiler, economizer and ejector are chosen for discussion because they have higher exergy destruction rates in comparison to others. Table 4 shows the result of system simulation. Table 5 shows the performance of the system. It is found that energy and exergy efficiencies of the proposed CECP system are 24.4% and 9.8%, respectively.

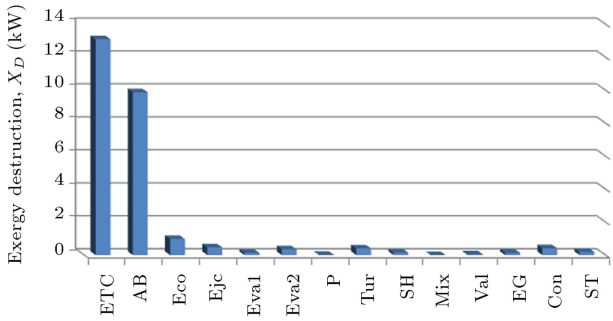

Figure 2. Components exergy destruction rate in CECP cycle.

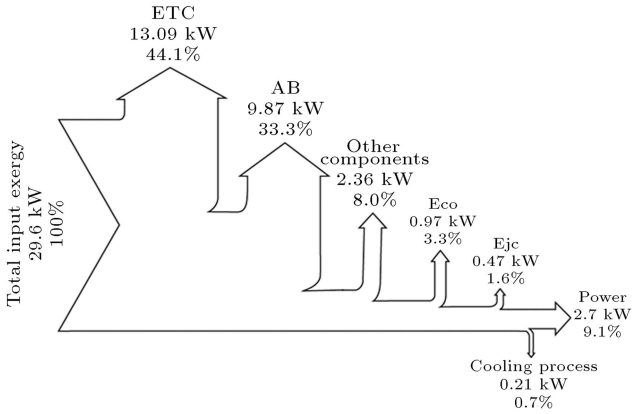

Figure 3. The Grassman diagram of components exergy destruction as a percentage of total input exergy ($X_{\mathrm{in},t} = 29.6$ kW).

5.1. Overall efficiency and exergy destruction

The solar CECP system components exergy destruction rates, exergy efficiencies and their percentages as total exergy destructed and total exergy input are shown in Table 6. Table 6 and Figures 2 and 3 illustrate that solar collector and auxiliary boiler are the major sources of exergy destruction. The solar collector destroys 13.09 kW (49.9% of total exergy destruction and 44.2% of total exergy input) and the auxiliary boiler destroys 9.87 kW (37.6% of total exergy destruction and 33.3% of total exergy input). In contrast, the exergy destructed by remaining components is lower. In figure 3, the Grassmann diagram demonstrates that power and cooling load exergies are 9.1% and 0.7% of total exergy input. Moreover, it indicates that the most significant components that have high destruction rates in system are solar collector and auxiliary boiler. Therefore, careful design and selection of these two components are essential in designing a solar CECP system.

5.2. Effect of turbine inlet pressure

The effect of turbine inlet pressure on CECP system efficiencies and components exergy destruction rates is

Table 3. Comparison between the model and the literature.

	m (kg s^{-1})			T (°C)			P (kPa)		
	Literature	Model	Difference %	Literature	Model	Difference %	Literature	Model	Difference %
1	4.549	4.66	2.40%	130	130	0%	700	700	0%
2	1.765	1.817	2.95%	98.98	98.98	0%	220	220	0%
3	2.647	2.843	7.40%	78.73	84.69	7.60%	91.4	109.7	20%
4	1.902	1.959	3%	89.88	90.33	0.50%	91.4	109.7	20%
5	4.549	4.802	5.56%	83.41	87	4.30%	91.4	109.7	20%
6	4.549	4.802	5.56%	25	30	20%	91.4	109.7	20%
7	0.137	0.1418	3.50%	25	30	20%	91.4	109.7	20%
8	0.137	0.1418	3.50%	-5	-5	0%	25.8	25.9	0.40%
9	0.137	0.1418	3.50%	-5	-5	0%	25.8	25.9	0.40%
10	4.549	4.66	2.44%	25	30	20%	91.4	109.7	20%
11	4.549	4.66	2.44%	25.35	30.34	19.70%	700	700	0%
14	20	20	0%	140	140	0%	700	700	0%
17	20	20	0%	98.24	127	29.30%	700	700	0%
21	100	100	0%	20	20	0%	101	101	0%
22	100	100	0%	21.94	22.4	2.10%	101	101	0%
NRMSD		0.12%			5.6%			1.72%	

Table 4. Result of system simulation.

state	Fluid	m (kg s^{-1})	T (°C)	P (kPa)	h (kJ kg^{-1})	s (kJ kg^{-1} K^{-1})	x (kJ kg^{-1})	X (kW)
1	R123, superheated	0.097	130	1000	466.3	1.7438	52.37	5.08
2	R123, superheated	0.049	94.15	300	446.3	1.7507	30.33	1.49
3	R123, superheated	0.049	68.24	91.48	429.6	1.7658	9.248	0.45
4	R123, superheated	0.078	57.01	91.48	421.1	1.7409	8.009	0.62
5	R123, superheated	0.126	61.34	91.48	424.4	1.7505	8.456	1.07
6	R123, saturated liquid	0.126	25	91.48	226.2	1.0914	0.2	0.03
7	R123, saturated liquid	0.029	25	91.48	226.2	1.0914	0.2	0.0058
8	R123, saturated mixture	0.029	-5	25.9	226.2	1.0978	-1.635	-0.05
9	R123, saturated vapor	0.029	-5	25.9	379.6	1.6695	-13.01	-0.38
10	R123, saturated liquid	0.097	25	91.48	226.2	1.0914	0.2	0.02
11	R123, compressed liquid	0.097	25.57	1000	227.1	1.0923	0.832	0.08
12	R123, saturated liquid	0.097	111.1	1000	321.8	1.3691	15.83	1.54
13	R123, saturated vapor	0.097	111.1	1000	448.4	1.6986	47.46	4.60
14	Water, compressed liquid	0.2	140	1000	589.7	1.7387	90.25	18.05
15	Water, compressed liquid	0.2	138	1000	581	1.7193	87.14	17.43
16	Water, compressed liquid	0.2	123.6	1000	519.6	1.5656	70.04	14.01
17	Water, compressed liquid	0.2	112.7	1000	473.6	1.4481	57.92	11.58
18	Water, compressed liquid	0.2	126.4	1000	530.9	1.5954	72.8	14.56
19	Water, compressed liquid	0.25	126.4	1000	531.4	1.5954	73.32	18.33
20	Water, compressed liquid	0.25	137.5	1000	578.8	1.7124	87	21.75
21	Water, compressed liquid	0.4	15	300	63.2	0.2242	0.2	0.08
22	Water, compressed liquid	0.4	29.97	300	125.8	0.4360	1.772	0.71
23	Water, compressed liquid	0.215	5	300	21.32	0.0763	0.945	0.20
24	Water, compressed liquid	0.215	0	300	0.264	0	1.9	0.41

examined through Figures 4 and 5. It can be observed that both energy and exergy efficiencies increase as turbine inlet pressure increases while required collector area decreases. Energy efficiency improves within 53% because of decrement of heat provided by solar collector; exergy efficiency has the same improvement

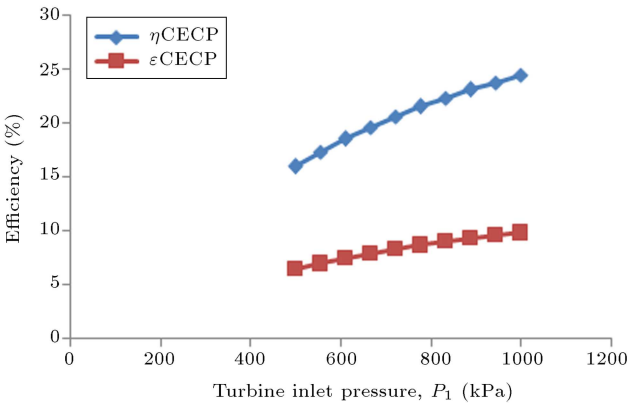

Figure 4. Effect of turbine inlet pressure on the energy and exergy efficiencies of the system.

Table 5. Result of thermodynamic simulation.

Required collector surface area (m^2)	15.31
Turbine inlet mass flow rate (kg s^-1)	0.097
Ejector entrainment ratio	0.6
Total heat required (kW)	23.22
Total exergy input (kW)	29.6
Thermal efficiency (%)	24.4
Exergy efficiency (%)	9.8

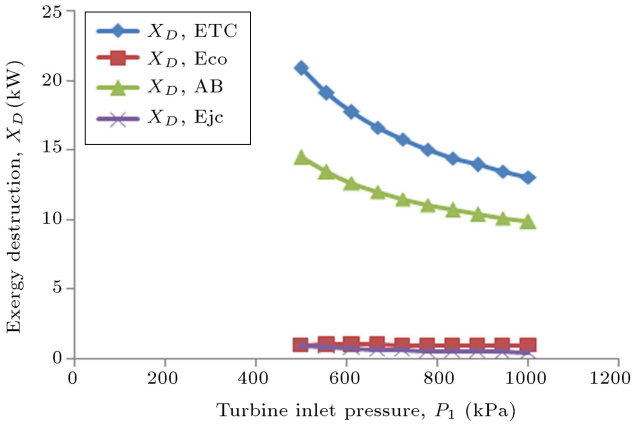

Figure 5. Effect of turbine inlet pressure on components exergy destruction rates.

due to the decrement of components exergy destructions. Figure 5 demonstrates that solar collector and auxiliary boiler exergy destruction rate is more sensitive to turbine inlet pressure in comparison to economizer and ejector exergy destruction rates. The sensitivity is because solar exergy increases widely because of changes in collector area, and consequently solar collector exergy destruction rate drops from 20.9 kW to 13 kW. In auxiliary boiler, this variation is owing to decrement in auxiliary boiler inlet and outlet exergy difference, while economizer and ejector exergy destruction rates are almost constant because of slight changes in the exergy streams.

5.3. Effect of turbine inlet temperature

The effect of turbine inlet temperature on CECP system efficiencies, and components exergy destruction

Table 6. Comparative result of exergy analysis of components.

Components	Exergy destruction rate, X_D (kW)	Exergy efficiency (%)	$X_{D,c}/X_{D,t}$ (%)	$X_{D,c}/X_{\text{in},t}$ (%)
Tur	0.40	87	1.5	1.4
Ejc	0.47	57	1.8	1.6
Eva1	0.13	62	0.5	0.4
Evap2	0.35	90	1.3	1.2
P	0.02	71	0.08	0.1
Eco	0.97	60	3.7	3.3
SH	0.15	77	0.6	0.5
Con	0.41	60	1.6	1.4
Mix	0.004	-	0.02	0.01
Va	0.05	-	0.2	0.2
EG	0.14	95	0.5	0.5
AB	9.87	65	37.6	33.3
ST	0.18	99	0.7	0.6
ETC	13.09	21	49.9	44.2
CECP	26.234	9.8	100	-

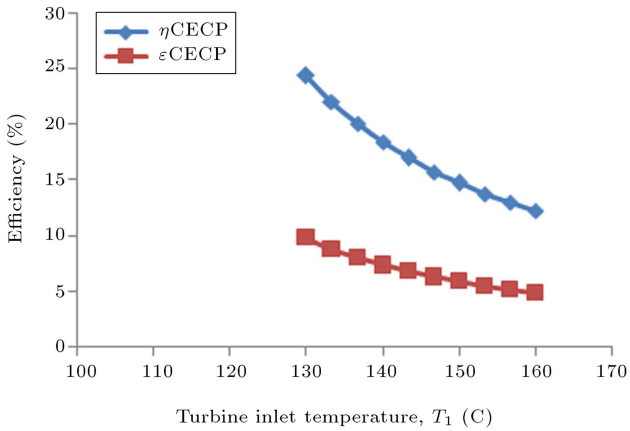

Figure 6. Effect of turbine inlet temperature on the energy and exergy efficiencies of the system.

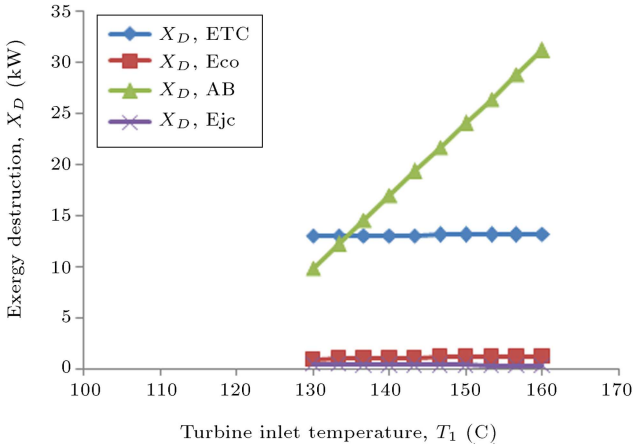

Figure 7. Effect of turbine inlet temperature on components exergy destruction rate.

rates is illustrated through Figures 6 and 7. Figure 6 reveals that increment turbine inlet temperature decreases energy and exergy efficiencies of the system within 50%. Energy efficiency decreases because of increasing the requirement of total heat provided, and exergy efficiency decreases due to components exergy destruction rates increment. Figure 7 illustrates the effect turbine inlet temperature on components exergy destruction rates. As the turbine inlet temperature increases, auxiliary boiler exergy destruction rate increases. By increasing turbine inlet temperature, auxiliary boiler outlet temperature increases, therefore both outlet exergy stream of the auxiliary boiler and the amount of fuel required in the auxiliary boiler increase, but the increment in the product exergy of the auxiliary boiler is more than in fuel exergy, and as a result exergy destruction rate increases. Solar collector exergy destruction rate remains almost constant due to consistency in collector area and as a result in solar exergy. Ejector exergy destruction rates decreases within 19% due to decrement in outlet exergy stream of ejector. Economizer exergy destruction increases from 0.97 kW to 1.3 kW because of increasing of difference between inlet and outlet exergy streams.

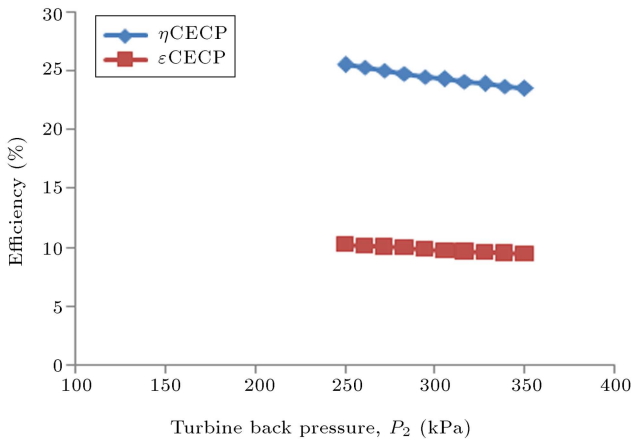

Figure 8. Effect of turbine back pressure on energy and exergy efficiencies of the system.

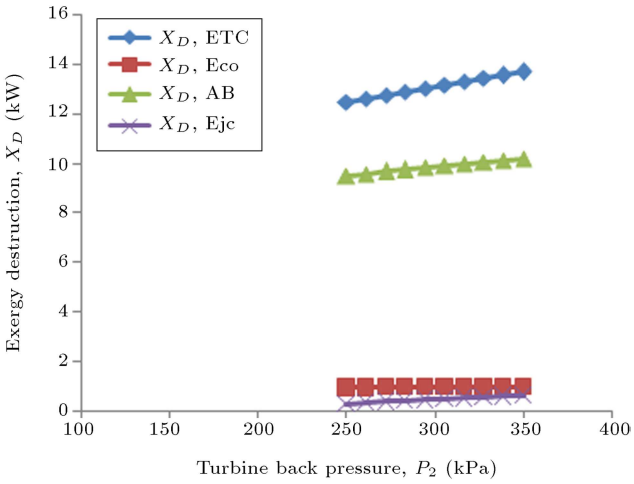

Figure 9. Effect of turbine back pressure on components exergy destruction rates.

5.4. Effect of turbine back pressure

In this subsection, CECP system efficiencies, required collector area and components exergy destruction rates versus turbine back pressure variations are investigated through Figures 8 and 9. The study shows that increasing turbine back pressure decreases energy and exergy efficiencies slightly. Energy efficiency decreases within 8% due to slight change in total heat required, and exergy efficiency also decreases within 8% because of slight change in components exergy destruction rates.

Figure 9 illustrates the variation of components exergy destruction rate against turbine back pressure variation. It is revealed that increasing turbine back pressure increases all components exergy destruction rates slightly.

6. Optimization method using genetic algorithm

The genetic algorithm is based on the natural selection theory in the biological genetic progress developed by Charles Darwin and introduced firstly by John Holland [39]. In the GA, every parameter is considered as a gene and a solution is considered as a chromosome and they are encoded as binary numbers. A population of variable chromosome like structure is built by various combinations of genes. A group of chromosomes are given, which is called the original population, before the GA theory is applying. The better approximations in the original population generate a new generation and the better approximations to potential results are selected as the new population. Then the new population continues to generate next generation and stops when the population converges to the optimal result. In the GA, the fitness function evaluates the fitness value, and large fitness value results better adaptability of the chromosome-like structure. In this investigation, the energetic and exergetic system efficiencies are chosen as the fitness function.

7. Optimization results

Table 7 indicates the various key thermodynamic parameters and the operation parameters of GA, in this solar-driven ejector cooling and power system. The maximum and minimum values of turbine inlet pressure is set to be 500-1000 kPa to enable the system to operate stably and the range of inlet temperature of turbine 130-160°C. Table 8 represents the results of parameter optimization for the optimum values of objective functions. It is found that to achieve the optimal energetic and exergetic efficiencies, separately, turbine inlet pressure is close to the maximum value and turbine inlet temperature and back pressure are close to their saturated values. In the other words, under the actual constraints, a higher turbine inlet pressure with low temperature vapor state in turbine outlets could obtain a better system performance of solar driven ejector cooling and power generation system.

Table 7. Parameter optimization in GA.

Population size	10
Crossover probability	0.8
Mutation probability	0.02
Stop generation	200
The range of turbine inlet pressure, P_1 (kPa)	500-1000
The range of turbine inlet temperature, T_1 (C)	130-160
The range of turbine back pressure, P_2 (kPa)	250-350

Table 8. Optimization results of solar driven CECP system.

Objective function		**P_1 (kPa)**	**T_1 (C)**	**P_2 (kPa)**
ηCECP (%)	**25.43**	998.7	130.03	252.3
εCECP (%)	**10.18**	999.5	130.06	255.2

8. Conclusion

In this study, a solar CECP system is proposed for specified amount of electricity and cooling. Required collector area and solar fraction are calculated considering day in July maximum monthly average daily radiation. Energy and exergy analysis of this system is conducted. Moreover overall exergy destruction rate of system and each component is calculated. Performance of system is examined by varying key parameters such as turbine inlet pressure, turbine inlet pressure and turbine back pressure. Finally, genetic algorithm is employed to conduct the parameter optimization with the exergy efficiency as its objective function. The following remarks can be concluded from this study:

- Energy and exergy efficiencies of the system are calculated to be 24.4% and 9.8%, respectively.
- Amount of required collector area and solar fraction are calculated to be 16.32 m^2 and 0.5, respectively.
- It is found that, auxiliary boiler and solar collector are the main exergy destruction sources. Thus for increasing system exergetic performance it is essential to have careful design of these components.
- Energy and exergy efficiencies may improve up to 53% by increasing turbine inlet pressure, while they decrease down to 50% by increasing turbine inlet temperature and 8% by increasing turbine back pressure.
- Exergy destruction rates of solar collector and auxiliary boiler decreases by increasing the turbine inlet pressure, while it increases by increasing turbine inlet temperature and turbine back pressure.
- Optimization of the system using GA improves the energy and exergy efficiencies up to 25.43% and 10.18%, respectively.

Nomenclature

A	Surface area of solar collector, m^2
C_p	Specific heat, kJ kg^{-1} K^{-1}
G	Total instantaneous radiation, W m^{-2}
h	Specific enthalpy, kJ kg^{-1}
H	Monthly average radiation, J m^{-2}

K_T	Monthly average clearness index
L	Latitude, °
LHV	Lower Heating Value, kJ
m	Mass flow rate, kg s^{-1}
N	Day number
P	Pressure, kPa
Q	Heat, kW
R	Tilt factor
W	Power, kW
x	Specific exergy, kJ kg^{-1}
X	Exergy rate, kW

Subscripts

a	Average
b	Beam
CH	Chemical
CL	Cooling load
D	Destruction
d	Diffuse
dif	Ejector diffuser
e	Exit
$e1$	Outlet of the ejector nozzle
$e2$	Mixing section of the ejector
f	Fuel
i	Inlet
is	Isentropic
KN	Kinetic
L	Loss
m	Ejector mixer
NRMSD	Normalized Root-Mean-Square Deviation
n	Ejector nozzle
O	Extraterrestrial
PH	Physical
PT	Potential
R	Reflected
s	Sun
sc	Solar constant, W/m^2
SS	sunset
t	Tilt
u	Useful
0	Dead state

Greek symbols

ρ	Ground albedo
η	Thermal efficiency (%)
ε	Exergy efficiency (%)
δ	Declination angle, °
β	Slope angle of the collector, °
ν	Specific volume, m^3/kg
ω	Hour angle, °
μ	Entrainment ratio

References

1. Goswami, D. "Solar thermal power: Status of technologies and opportunities for research, heat and mass transfer", *2nd ASME-ISHMT Heat and Mass Transfer Conference*, Tata-McGraw Hill Publishers, New Delhi, India, pp. 57-60 (1995).
2. Yogi Goswami, D. "Solar thermal power technology: present status and ideas for the future", *Energy Sources*, **20**(2), pp. 137-145 (1998).
3. Xu, F., Yogi Goswami, D. and S. Bhagwat, S. "A combined power/cooling cycle", *Energy*, **25**(3), pp. 233-246 (2000).
4. Vijayaraghavan, S. and Goswami, D.Y. "On evaluating efficiency of a combined power and cooling cycle", *ASME 2002 International Mechanical Engineering Congress and Exposition*, American Society of Mechanical Engineers, pp. 287-295 (2002).
5. Hasan, A.A. and Goswami, D. "Exergy analysis of a combined power and refrigeration thermodynamic cycle driven by a solar heat source", *Journal of Solar Energy Engineering*, **125**(1), pp. 55-60 (2003).
6. Lu, S. and Goswami, D.Y. "Optimization of a novel combined power/refrigeration thermodynamic cycle", *ASME Solar 2002: International Solar Energy Conference*, American Society of Mechanical Engineers, pp. 75-82 (2002).
7. Tamm, G. and Goswami, D.Y. "Novel combined power and cooling thermodynamic cycle for low temperature heat sources. Part II: Experimental investigation", *Journal of Solar Energy Engineering*, **125**(2), pp. 223-229 (2003).
8. Tamm, G., Hasan, A.A., Goswami, D.Y. and Lu, S. "Novel combined power and cooling thermodynamic cycle for low temperature heat sources. Part I: Theoretical investigation", *Journal of Solar Energy Engineering*, **125**(2), pp. 218-222 (2003).
9. Sadrameli, S. and Goswami, D. "Optimum operating conditions for a combined power and cooling thermodynamic cycle", *Applied Energy*, **84**(3), pp. 254-265 (2007).
10. Padilla, R.V., Demirkaya, G., Goswami, D.Y., Stefanakos, E. and Rahman, M.M. "Analysis of power and cooling cogeneration using ammonia-water mixture", *Energy*, **35**(12), pp. 4649-4657 (2010).
11. Amano, Y., Suzuki, T., Hashizume, T., Akaiba, M., Tanzawa, Y. and Usui, A. "A hybrid power generation and refrigeration cycle with ammonia-water mixture",

Proceedings of 2000 International Joint Power Generation Conference, Miami, pp. 23-26 (2000).

12. Takeshita, K., Amano, Y. and Hashizume, T. "Demonstration of a hybrid power and refrigeration ammonia-water cycle", *ASME Turbo Expo 2006: Power for Land, Sea, and Air*, American Society of Mechanical Engineers, pp. 469-474 (2006).
13. Zheng, D., Chen, B., Qi, Y. and Jin, H. "Thermodynamic analysis of a novel absorption power/cooling combined-cycle", *Applied Energy*, **83**(4), pp. 311-323 (2006).
14. Zheng, D.-X., Chen, B., Qi, Y. and Jin, H.-G. "A thermodynamic analysis of a novel absorption power/cooling combined cycle", *Journal of Engineering Thermophysics*, **23**(5), pp. 539-542 (2002).
15. Zhang, N., Cai, R. and Lior, N. "A novel ammonia-water cycle for power and refrigeration cogeneration", *ASME 2004 International Mechanical Engineering Congress and Exposition*, American Society of Mechanical Engineers, pp. 183-196 (2004).
16. Zhang, N. and Lior, N. "Methodology for thermal design of novel combined refrigeration/power binary fluid systems", *International Journal of Refrigeration*, **30**(6), pp. 1072-1085 (2007).
17. Zhang, N. and Lior, N. "Development of a novel combined absorption cycle for power generation and refrigeration", *Journal of Energy Resources Technology*, **129**(3), pp. 254-265 (2007).
18. Liu, M. and Zhang, N. "Proposal and analysis of a novel ammonia-water cycle for power and refrigeration cogeneration", *Energy*, **32**(6), pp. 961-970 (2007).
19. Nord, J., Lear, W., and Sherif, S. "Analysis of heat-driven jet-pumped cooling system for space thermal management", *Journal of Propulsion and Power*, **17**(3), pp. 566-570 (2001).
20. Wang, J., Dai, Y. and Gao, L. "Parametric analysis and optimization for a combined power and refrigeration cycle", *Applied energy*, **85**(11), pp. 1071-1085 (2008).
21. Wang, J., Dai, Y., Zhang, T. and Ma, S. "Parametric analysis for a new combined power and ejector-absorption refrigeration cycle", *Energy*, **34**(10), pp. 1587-1593 (2009).
22. Jawahar, C., Saravanan, R., Bruno, J.C. and Coronas, A. "Simulation studies on gax based Kalina cycle for both power and cooling applications", *Applied Thermal Engineering*, **50**(2), pp. 1522-1529 (2013).
23. http://www.fchart.com, Engineering Equation Solver (EES).
24. Cengel, A.Y. and Boles, M.A., *Thermodynamics: An Engineering Approach*, McGraw Hill, New York, (2008).
25. Ouzzane, M. and Aidoun, Z. "Model development and numerical procedure for detailed ejector analysis and design", *Applied Thermal Engineering*, **23**(18), pp. 2337-2351 (2003).
26. Huang, B.J., Chang, J.M., Wang, C.P. and Petrenko, V.A. "A 1-D analysis of ejector performance", *International Journal of Refrigeration*, **22**(5), pp. 354-364 (1999).
27. Dai, Y., Wang, J. and Gao, L. "Exergy analysis, parametric analysis and optimization for a novel combined power and ejector refrigeration cycle", *Applied Thermal Engineering*, **29**(10), pp. 1983-1990 (2009).
28. Kalogirou, S., *Solar Energy Engineering: Processes and Systems*, Elsevier, UK (2009).
29. Zhang, W., Ma, X., Omer, S.A. and Riffat, S.B. "Optimum selection of solar collectors for a solar-driven ejector air conditioning system by experimental and simulation study", *Energy Conversion and Management*, **63**(0), pp. 106-111 (2012).
30. http://www.apricus.com.au/downloads/, Apricus Collector Specifications.
31. Wang, M., Wang, J., Zhao, Y., Zhao, P. and Dai, Y. "Thermodynamic analysis and optimization of a solar-driven regenerative organic Rankine cycle (ORC) based on flat-plate solar collectors", *Applied Thermal Engineering*, **50**(1), pp. 816-825 (2013).
32. Kotas, T.J., *The Exergy Method of Thermal Plant Analysis*, Krieger Pub., Malabar, Fla. (1995).
33. Bejan, A., Tsatsaronis, G. and Moran, M.J., *Thermal Design and Optimization*, John Wiley & Sons Inc., New York (1996).
34. Kaviri, A.G., Jaafar, M.N.M. and Lazim, T.M. "Modeling and multi-objective exergy based optimization of a combined cycle power plant using a genetic algorithm", *Energy Conversion and Management*, **58**(0), pp. 94-103 (2012).
35. Al-Sulaiman, F.A., Dincer, I. and Hamdullahpur, F. "Exergy modeling of a new solar driven trigeneration system", *Solar Energy*, **85**(9), pp. 2228-2243 (2011).
36. Wang, J., Dai, Y., Gao, L. and Ma, S. "A new combined cooling, heating and power system driven by solar energy", *Renewable Energy*, **34**(12), pp. 2780-2788 (2009).
37. Paul W. Stackhouse, J., Ph.D., https://eosweb.larc.nasa.gov/cgi-bin/sse/sse. cgi (2013).
38. Wang, J., Dai, Y. and Sun, Z. "A theoretical study on a novel combined power and ejector refrigeration cycle", *International Journal of Refrigeration*, **32**(6), pp. 1186-1194 (2009).
39. Holland, J., *Adaptation in Natural and Artificial Systems*, University of Michigan Press, Ann Arbor (1975).

Biographies

Fateme Ahmadi Boyaghchi received her BSc degree in Mechanical Engineering, Iran, and MSc and PhD degrees in Energy Conversion all from Iran University

of Science and Technology. Her specific research interest is solar-driven energy systems, environment and conventional power plants. She has two books and numerous professional journal articles. She is currently assistant professor in the Faculty of Engineering at Alzahra University, Iran.

Parisa Heidarnejad received her BSc in Mechanical Engineering from Urmia University, Urmia Iran, in 2010, and is currently an MSc student of Energy systems in the Faculty of Engineering at Alzahra University, Iran. Her research interests include solar energy systems and optimization.